G. Cliche
F. Bonn
*Département de géographie*
*Université de Sherbrooke*
*Sherbrooke, Québec J1K 2R1, Canada*
P. Teillet
*Canada Centre for Remote Sensing*
*Ottawa, Ontario K1A 0Y7, Canada*

# Integration of the SPOT Panchromatic Channel into Its Multispectral Mode for Image Sharpness Enhancement

It is possible to increase the visual spatial resolution of SPOT multispectral data, giving rise to a product which is very similar to a color infrared aerial photograph.

Abstract: *By integrating* SPOT*'s panchromatic channel with 10-m resolution into its multiband channels with 20-m resolution, it is possible to produce a high resolution image suitable for photo interpretation.*

*Three different integration algorithms have been tested on simulated* SPOT *data in order to produce color composite images using* SPOT*'s multispectral mode (three channels) in combination with its 10-m resolution panchromatic mode. The algorithm that gave the best visual results used a different integration formula for the near infrared channel than for the green and red channels, due to the fact that the panchromatic is less correlated with the infrared than with the visible channels.*

*The result looks very similar to a color infrared air-photo with high resolution and good spectral information quality.*

## Introduction

The SPOT (Système Probatoire d'Observation de la Terre) satellite system, scheduled for launch by France in 1985, will be equipped with two HRV (Haute Résolution Visible) pushbroom sensors, which may work either in a panchromatic mode with 10-m resolution or in a multispectral mode in three channels with 20-m resolution. These characteristics will allow SPOT to be the civilian remote sensing satellite with the best spatial resolution in the 1980s.

Among the innovative features of this future satellite, SPOT will have the capability of viewing up to 27° off-nadir, thereby allowing stereoscopic imaging from two different orbits. A sequence of recorded images for a specific area may include both modes of instrument operation (multispectral or panchromatic) (CNES, 1980).

For this reason, we have integrated images of an area taken in both modes, resulting in a product of very high resolution and with good spectral content which can be used for visual interpretation as a color infrared air-photo.

## Data Acquisition

The original data were acquired with an 11-channel Daedalus DS-1260 multispectral scanner (MSS) flown at 4875-m altitude on a Falcon Jet of the Canada Centre for Remote Sensing (CCRS). The flight took place in good atmospheric conditions over the city of Sherbrooke, Québec, in June of 1982.

The Daedalus scanner measures radiance from ground elements in 11 spectral bands in the visible and near infrared portion of the spectrum (Zwick *et al.*, 1980). It scans with a 37° maximum angle from nadir. In comparison, SPOT will have an angular field of view of 4°, besides its off-nadir viewing capability of 27°. Therefore, airborne simulations will never



0099-1112/85/5103-0311$02.25/0

be able to reproduce exactly the satellite image, because viewing angles on the simulation vary from pixel to pixel along the same scan line. This limitation has to be kept in mind for all further work on simulated images.

## Simulation of SPOT Data

All the processing tasks for obtaining simulated SPOT data and the integration of panchromatic and multispectral data were performed on the CCRS Image Analysis System (CIAS) (Goodenough, 1979).

### Spectral Simulation

Individual SPOT channels cover a wider part of the spectrum than do airborne MSS channels. Thus, a simulation of SPOT spectral responses requires a combination of appropriate MSS channels. Simard (1981) has generated weighting coefficients related to the differential responsivity of SPOT and airborne MSS channels. Corrected by Ahern (1982) in order to take gain into account, these coefficients have been used to put suitable weightings on the MSS channels. In particular, channels 3, 4, 5, 6, 7, and 8 have been used to simulate the SPOT panchromatic channel, designated $P$; channels 4 and 5 to simulate the SPOT green channel, designated $S_1$; channels 6 and 7 for the SPOT red channel, designated $S_2$; and channel 9 for the SPOT infrared channel, designated $S_3$ (Table 1).

### Spatial Simulation

To simulate the spatial resolution of channels $S_1$, $S_2$, and $S_3$, which will be 20 m on SPOT, the input pixels of 10 by 12 m were resampled using a truncated $(\sin x)/x$ convolution to assure that straight lines would appear smoother and edges sharper (Moik, 1980). This results in a pixel size of 20 by 24 m for the multispectral channels ($S_i$) while the original 10 by 12 m pixel is used for the panchromatic channel $P$. These pixel sizes are considered to be close enough to the size of SPOT pixels for the purpose of this study, which does not require area measurements or geometric accuracy (Figure 1 and Plate 1).

A sub-image of 512 by 512 pixels in the panchromatic mode (or 256 by 256 in the multispectral mode) was used because of the display limitation of the CIAS monitor. Each multispectral pixel, $S_i$, corresponds to four panchromatic pixels, $P$ (Figure 2).

## Integration of Panchromatic and Multispectral Modes

Integration of the high resolution panchromatic channel and the lower resolution multispectral channels has the purpose of incorporating increased spatial information into the multispectral channels.

The integration technique is similar to that used by Wong and Orth (1980) for integrating Landsat MSS and Seasat synthetic aperture radar images. The method consists in modulating the intensity of each MSS channel, having a spatial resolution of 50 m after resampling, with the black-and-white Seasat image with a 25-m resolution. The modulated channels 4, 5, and 7 are then used to produce a color composite image with the high resolution of the Seasat image and the spectral content of the Landsat image.

We have tested different algorithms in order to find a method yielding imagery closely resembling color infrared photography, which would allow visual interpretation of spaceborne data by users lacking digital analysis facilities.

Three integration algorithms were tested:

(a) Square root of the product $P \times S_i$, under the general form
$A_a * (P * S_i)^{1/2} + B_a$.

(b) Product $P \times S_i$, compensated by gain and offset, under the general form
$A_b * (P * S_i) + B_b$.

(c) The best results were obtained by using
$A_1 * (P * S_1)^{1/2} + B_1$ for blue,
$A_2 * (P * S_2)^{1/2} + B_2$ for green, and
$A_3 * (0.25P + 0.75\,S_3) + B_3$ for red.

Table 1. Wavelengths of SPOT and Airborne MSS Channels (in Nanometres), and Corresponding Weighting Coefficients (adapted from Simard, (1981))

| Airborne MSS | SPOT Multispectral | Weighting coefficients | SPOT Panchromatic | Weighting coefficients |
|---|---|---|---|---|
| 1 390–415 | | | | |
| 2 415–450 | | | | |
| 3 445–495 | | | $P$ (495–730) | 0.005 |
| 4 500–550 | $S_1$ (497–585) | 0.595 | | 0.280 |
| 5 550–595 | | 0.405 | | 0.237 |
| 6 590–645 | $S_2$ (616–675) | 0.255 | | 0.172 |
| 7 625–695 | | 0.745 | | 0.217 |
| 8 680–780 | | | | 0.089 |
| 9 765–895 | $S_3$ (788–894) | 1.00 | | |
| 10 865–1003 | | | | |
| 11 1550–1750* | | | | |

* Optional


FIG. 1. Simulation of SPOT panchromatic channel imagery with 10-m resolution over the city of Sherbrooke, Quebec.


PLATE 1. Simulation of SPOT multispectral channel imagery with 20-m resolution.

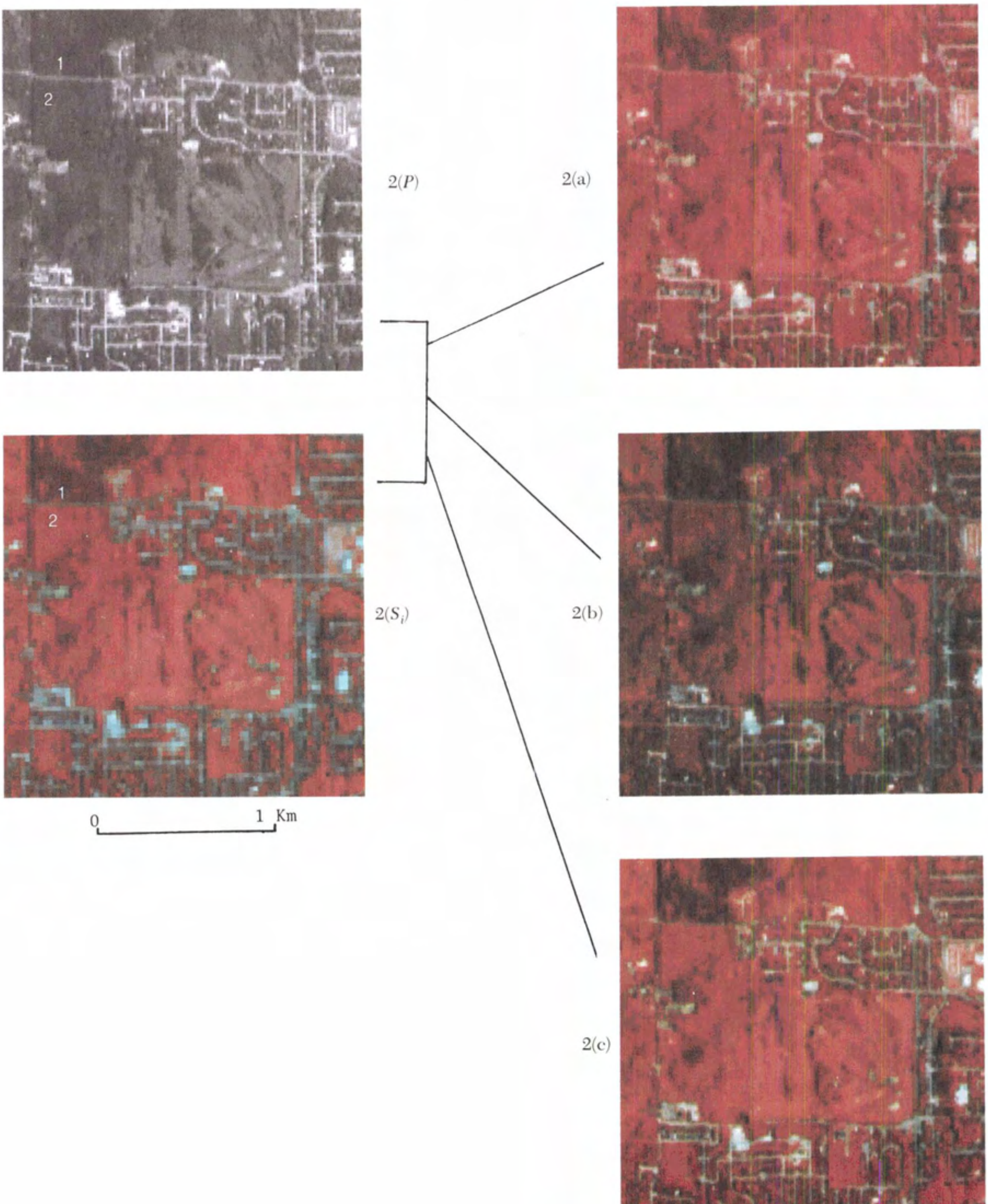


PLATE 2. Sub-images comparing the results 2(a), 2(b), and 2(c) after algorithms a, b, and c were performed on the panchromatic channel and the multispectral channels 2(*P*) and 2($S_i$), respectively.

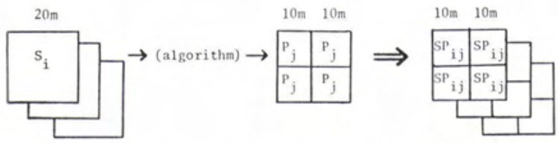


FIG. 2. Schematic representation of the integration process.

The *algorithm* (*a*), used to produce the integrated $PS_i$, was expected to be the best because each channel, $P$ and $S_i$, is a function of the reflectivity such that $P * S_i$ is proportional to (reflectivity)$^2$ while the square root of this product preserves all the pixel values within the full dynamic range.

In order to remain within the dynamic range (0-255), the constant $A_b$ of *algorithm* (*b*) must be small. However, this had the effect of concentrating the pixel values in the lower part of the reflectivity histogram, which produces a dark image with poor contrast.

*Algorithm* (*c*) used the same method as algorithm (a) to integrate bands $S_1$ and $S_2$, and has the advantage of reducing the weight of the panchromatic channel when it is integrated with the infrared channel. This takes into account the fact that the correlation between the infrared channel, $S_3$, and the panchromatic channel, $P$, is lower than the correlation between the panchromatic and the visible channels $S_1$ and $S_2$. In images for visual interpretation, as in digital analysis, it is suggested that the infrared information be kept uncoupled from the information in the visible bands.

By reducing the weight of the panchromatic channel in its integration with $S_3$, the resulting band, $PS_3$, looks more like an infrared channel and, therefore, is little correlated with the visible bands.

However arbitrary, the weights used for the panchromatic and infrared channels ($P$ and $S_3$) increase the spatial resolution from 20 to 10 m and preserve much of the infrared information (see Cover Photo).

## RESULTS AND DISCUSSION

Plate 2 shows a sub-image centered on Sherbrooke's Golf Club. A comparison of Plate 2(*P*) (panchromatic with a 10-m pixel) and Plate 2($S_i$) (multispectral mode at 20 m) shows the fine details channel $P$ will provide and the usefulness of the multispectral mode for discriminating terrain features. Note in Plate 2(*P*) the sharp definition of the streets and in Plate 2($S_i$) the clear discrimination between two land-use classes (softwood (1) and pasture (2)).

Plates 2(a), 2(b), and 2(c) illustrate the three resulting images after the application of each of the three test algorithms (a, b, and c) in the integration process. In all three images, the fine resolution evident in 2(*P*) is preserved. With respect to spectral content, Plate 2(a) looks like a washed out image due to the fact that the algorithm used is the same for all $S_i$ channels and, thus, increases the correlation between the infrared and the visible bands. Plate 2(b) is too dark and has weak contrast, which makes the discrimination between features difficult. As expected from theory, Plate 2(c) gives the best result due to the use of a different algorithm for integrating channel $P$ into the infrared channel $S_3$, which helps to keep $S_3$ uncoupled from the visible bands and, thus, increases the visual information content on the color composite image. The sharp definition of features is maintained and the differentiation of various land-use types is as good as in Plates 2(*P*) and 2($S_i$), respectively.

## CONCLUSION

This study shows that it is possible to increase the visual spatial resolution of SPOT multispectral data by integrating the 10-m panchromatic channel and the 20-m multispectral channel, giving rise to a product which is very similar to a color infrared aerial photograph. Such a product will allow the use of spaceborne images by investigators familiar with visual photointerpretation and who have no facilities for digital analysis. The use of this type of imagery should even be greater with the stereo viewing capacity of SPOT.

## ACKNOWLEDGMENTS

The authors wish to thank Dr. David Horler of CCRS for his advice, Dr. Hugh Gwyn of Université de Sherbrooke for the revision of this paper, and the Québec Government for funding the data acquisition (Project F.C.A.C. EQ 102 and C.R.S.A.Q., # S-82-954).

## REFERENCES

Ahern, F. J., 1982. *Spectral Band Weights for SPOT and MSS Simulation.* CCRS Memorandum, July 29.

Centre National d'Études Spatiales, 1980. *SPOT système de télédétection par satellite,* brochure explicative. Centre spatial de Toulouse, Toulouse, France.

Goodenough, D. G., 1979. The Image Analysis System (CIAS) at the Canada Centre for Remote Sensing, *Canadian Journal of Remote Sensing,* Vol. 5, pp. 3-17.

Moik, J. G., 1980. *Digital Processing of Remotely Sensed Images,* NASA, Washington, D.C., Chapter 3.3.2.

Simard, R., 1981. Résultats de simulations d'images stéréoscopiques HRV SPOT sur le site de Gun Lake C.B., *Comptes rendus du septième symposium canadien de télédétection,* Winnipeg, Manitoba, pp. 541-551.

Wong, F. H., and R. Orth, 1980. Registration of SEASAT/LANDSAT composite images to UTM coordinates. *Proceedings of the Sixth Canadian Symposium on Remote Sensing,* Halifax, Nova Scotia, pp. 161-164.

Zwick, H. H., W. D. McColl, and H. R. Edel, 1980. The CCRS DS1260 airborne multispectral scanner (MSS), *Proceedings of the Sixth Canadian Symposium on Remote Sensing,* Halifax, Nova Scotia, pp. 643-648.

(Received 2 July 1983; revised and accepted 12 December 1984)